AJNR

Diffusion Tensor MR Imaging of Cerebral Gliomas: Evaluating Fractional Anisotropy Characteristics

M.L. White, Y. Zhang, F. Yu and S.A. Jaffar Kazmi

M.L. White
Y. Zhang
F. Yu
S.A. Jaffar Kazmi

Diffusion Tensor MR Imaging of Cerebral Gliomas: Evaluating Fractional Anisotropy Characteristics

BACKGROUND AND PURPOSE: FA correlation to glioma tumor grade has been mixed if not disappointing. There are several potential underlying fundamental issues that have contributed to these results. In an attempt to overcome these past shortfalls, we evaluated characteristics of FA of the solid tissue components of gliomas, including whether high-grade gliomas have a greater variation of FA than low-grade gliomas.

MATERIALS AND METHODS: Thirty-four patients with gliomas (9 grade II, 8 grade III, and 17 grade IV) underwent diffusion tensor imaging at 3T. Mean FA, maximum FA, and minimum FA values were measured within the solid tissue components of the tumors. The variations of FA were evaluated by determining the range of FA values and the maximum SDs of FA. The variations of FA values among different tumor grades were compared statistically. We also correlated FA variations with minimum FA and maximum FA.

RESULTS: The maximum FA, FA range, and maximum SD for grade II tumors were significantly lower than those for grade III and IV tumors ($P < .0001 \sim P = .0164$). A very good correlation of maximum FA to FA range ($r = 0.931$) and maximum SD ($r = 0.889$) was observed.

CONCLUSIONS: The FA range and maximum SD appear useful for differentiating low- and high-grade gliomas. This analysis added value to the findings on conventional MR imaging. In addition, focal maximum FA is a key factor contributing to the larger FA variation within high-grade gliomas.

ABBREVIATIONS: ANOVA = analysis of variance; ASSET = array spatial sensitivity encoding technique; FA = fractional anisotropy; FLAIR = fluid-attenuated inversion recovery; FSE = fast spin-echo; ROC = receiver operating characteristic analysis

G liomas are the largest group of primary cerebral neoplasms. Low-grade gliomas by conventional MR imaging are usually homogeneous without necrosis. Edema, hemorrhage, and contrast enhancement are relatively uncommon. High-grade gliomas, by contrast, present as inhomogeneous masses with edema, hemorrhage, and irregular contrast enhancement. Signs of frank cystic necrosis are highly suggestive of malignancy.[1,2] However, some high-grade tumors have relatively benign imaging features—homogeneous masses with minimal or no edema and little or no contrast enhancement.[3-5] Therefore, the presence or absence of cystic change, hemorrhage, edema, and contrast enhancement is not always specific for discriminating low-grade from high-grade tumors.

Recently, some studies have evaluated FA in cerebral gliomas by diffusion tensor imaging and have tried to determine whether FA values can be used to differentiate low- from high-grade gliomas. The results have been mixed if not disappointing. Inoue et al[6] stated that the mean FA values of low-grade gliomas were significantly lower than those of high-grade gliomas. Stadlbauer et al[7] reported lower mean FA values in higher grade gliomas with only a weakly significant difference. Also several studies have shown no significant difference for

mean FA between low- and high-grade gliomas.[8-10] Secondary to these conflicting results, mean FA values may not be useful for the preoperative grading of cerebral gliomas.

However, FA in gliomas has been found to be influenced by histologic characteristics and does correlate with cellularity, vascularity, cell density, neuronal and axonal structures, and fiber tracts.[11-14] Compared with low-grade gliomas, increased, sometimes focally, hypercellularity, cell density, and vascularity are found in high-grade gliomas. Some low-grade gliomas dedifferentiate into more malignant forms with time.[15-18] Potentially related to this process is that high-grade tumors sometimes present as malignant foci within an otherwise benign-appearing mass. Therefore, high-grade gliomas are histologically more heterogeneous (though potentially quite focally than low-grade gliomas. This feature is even without considering macroscopic tumor cystic change, necrosis, and hemorrhage. We hypothesized that the solid tissue components of high-grade gliomas would have a greater variation of FA values. To verify this hypothesis, we retrospectively reviewed diffusion tensor imaging studies in patients with gliomas and compared the FA variation of the different tumor grades. Additionally, this study analyzed the effectiveness of mean FA, maximum FA, and minimum FA values in the evaluation of tumor grade.

Materials and Methods

Patients

We (Y.Z., S.A.J.K.) searched the medical records and imaging database from our institution between April 2006 and July 2009. Thirty-

Subgroup of Gliomas ($N = 34$)		
	Grade II Gliomas ($n = 9$)	Grade III Gliomas ($n = 8$)	Grade IV Gliomas ($n = 17$)
Tumor type	Astrocytoma ($n = 4$)	Anaplastic astrocytoma ($n = 5$)	Glioblastoma ($n = 17$)
	Oligodendroglioma ($n = 4$)	Anaplastic oligodendroglioma ($n = 2$)	
	Pilomyxoid astrocytoma ($n = 1$)	Anaplastic oligoastrocytoma ($n = 1$)	
Age (yr)[a]	29.9 ± 18.8 (0.3–58)	52.9 ± 17.2 (36–90)	62.9 ± 8.4 (49–79)
Male/female	5:4	3:5	15:2

[a] Mean value ± SD. Numbers in parentheses are the range.

six consecutive patients with pathologically proved gliomas underwent pretreatment 3T MR imaging, including diffusion tensor imaging. Thirty-four were included in this retrospective study. The remaining 2 patients had grade IV tumors that presented as extensive necrotic areas surrounded by thin rings of enhancement without obvious solid components, and the FA of a solid-tissue component could not be measured. The pathologic diagnosis was determined with specimens removed at surgical resection ($n = 18$) or biopsy ($n = 16$) by a board-certified neuropathologist (S.A.J.K.) (Table). The interval between the preoperative MR imaging studies and the pathologic diagnosis was 1–36 days (mean, 7 days). Institutional review board approval was obtained, and informed patient consent was not required for the retrospective review of the medical records or the MR images for this study.

MR Imaging

MR imaging was performed on a 3T MR imaging unit (Signa HDx; GE Healthcare, Milwaukee, Wisconsin) with an 8-channel head coil. The gradient system was used in zoom mode with a gradient strength of 50 mT/m and a slew rate of 150 mT/m/s. Axial diffusion tensor imaging was performed by using a single-shot spin-echo echo-planar imaging sequence (TR, 9000; TE, 80.8; bandwidth, 250 kHz; matrix, 128 × 128 zero-filled to 256 × 256; FOV, 220 × 220 mm; section thickness, 3 mm; section gap, 0 or 0.5 mm; NEX, 1; ASSET factor, 2; b = 1000; directions of gradient sampling, 25). Studies obtained were associated with preoperative brain mapping MR imaging protocols that included thin-section axial T2-weighted images (TR, 3500; TE, 98.4; flip angle, 90°; bandwidth, 41.7 kHz; matrix, 256 × 256 zero-filled to 512 × 512; FOV, 250 × 250 mm; section thickness, 2 mm; section gap, 0 mm; NEX, 1; echo-train length, 18; ASSET factor, 2), thin-section postgadolinium axial T1-weighted FLAIR images (TR, 2026; TE, 9.2; TI, 883; bandwidth, 31.2 kHz; matrix, 256 × 256 zero-filled to 512 × 512; FOV, 250 × 250 mm; section thickness, 2 mm; section gap, 0 mm; NEX, 1; echo-train length, 5; ASSET factor, 2), and/or volumetric postgadolinium T1-weighted sagittal images (TR, 7.3; TE, 2.1; flip angle, 20°; bandwidth, 31.2 kHz; matrix, 256 × 256 zero-filled to 512 × 512; FOV, 250× 250 mm; section thickness, 1.6 mm; section gap, −0.8 mm; NEX, 1; ASSET factor, 2). These examinations were performed with a single dose of gadobenate dimeglumine ($n = 19$) (0.1 mmol/kg of body weight; MultiHance, Bracco, Milan, Italy) or gadopentate dimeglumine ($n = 15$) (0.1 mmol/kg of body weight; Magnevist, Schering, Berlin, Germany). Standard diagnostic MR imaging studies were available for comparison, which included pregadolinium sagittal T1-weighted, axial T1-weighted, axial T2-weighted FSE, axial T2-weighted FLAIR FSE, axial gradient-echo, and axial diffusion-weighted images. Postgadolinium axial and coronal T1-weighted images were also obtained.

MR Imaging Data Analysis

The MR images of these patients were analyzed in conference by a board-certified neuroradiologist (M.L.W.) and a radiologist (Y.Z.)

with knowledge of the diagnosis of glioma but without knowledge of the histologic grade. The radiologists reached a consensus regarding the imaging findings and region-of-interest determination. Areas evaluated were designated as whole tumor, enhanced tumor component, and nonenhanced tumor component. The maximum diameters of the tumors were recorded. The sensitivity and specificity of conventional MR imaging for preoperative grading were calculated. The preoperative grading had been made clinically before this study. Tumors without enhancement, edema, and necrosis were diagnosed as grade II gliomas. Tumors with inhomogeneous intensity, enhancement, and edema were diagnosed as grade III gliomas. Tumors that showed strong inhomogeneous enhancement and/or necrosis were diagnosed as grade IV gliomas.

All diffusion-tensor data were processed on a workstation (ADW 4.3, GE Healthcare) with FuncTool software (Version 4.5.1, GE Healthcare) for determining the FA measurements.

The mean FA of a tumor was measured by placing regions of interest on the FA maps in FuncTool software on the basis of the b = 0, b = 1000 isodiffusion, mean diffusivity maps, and conventional MR images. The 3D MR imaging spatial coordinates of tumor components delineated from the gadolinium-enhanced sequences were used to direct region-of-interest placement when needed in FuncTool. When measuring the mean FA, we drew regions of interest as large as possible to cover a maximum of tumor tissue without contacting the tumor border. Careful inspection of the images and cross-referencing of the 3D coordinates of tumor cysts, necrosis, and hemorrhage allowed us to avoid these structures. Ambiguous nonenhancing areas of tumor versus edema were not included in the analysis. All imaging sections that depicted tumor were selected for measuring FA. The mean tumor FA value represents averaged FA values from all image sections that contained tumor. This was calculated for the whole tumor, the enhanced component, and the nonenhanced component.

To evaluate the variation of FA, we calculated an FA range by subtracting the minimum FA from the maximum FA value measured in a tumor. Maximum SD of FA, which is supposed to reflect maximum histologic heterogeneity, was also measured. When measuring minimum FA, maximum FA, and maximum SD of FA, we used uniform ovoid regions of interest of approximately 30 mm^2 in obtaining measurements from the enhanced component, the nonenhanced component, and the whole tumor. An FA rainbow-colored map was used for analysis, which demonstrated the FA values in shades of blue, green, yellow, and red. The dark blue represented areas of low FA and the dark red represented areas of high FA. With visual inspection of the hue on FA maps, regions of interest were used to measure areas with high (red) or low (blue) FA values on each tumor section. From the values of these regions of interest, the highest or lowest one was chosen as the maximum or minimum FA of the corresponding areas of tumor, respectively. Areas with high contrast of hue (high FA variability) were measured to determine the SD of the FA. The largest SD measured was selected as the maximum SD of a tumor (Figs 1–4).
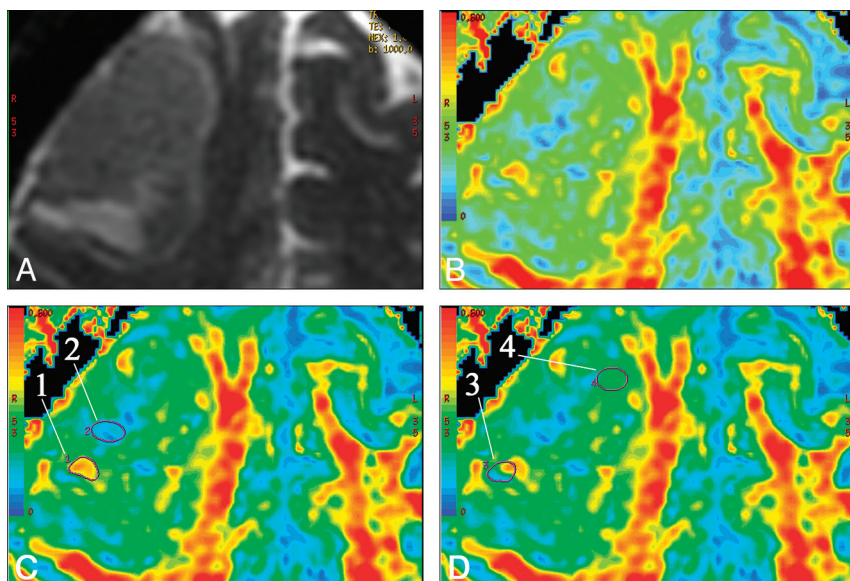
Fig 1. *A*, T2-weighted (*b* = 0) MR image shows a grade IV glioma in the right frontal lobe. *B*, FA map shows the different hues from blue to red in the tumor. *C* and *D*, FA maps at the same level show the method of region-of-interest selection. Region-of-interest 1 and region-of-interest 2 in *C* delineate red and blue areas that represent where the maximum FA and the minimum FA were measured. Region-of-interest 3 includes both blue and red portions and has a high contrast of color hue. The maximum SD is measured by region-of-interest 3 (SD = 0.125). The areas with homogeneous color hue have a low SD of FA. Region-of-interest 4 is an example of an area with a low SD (0.028).
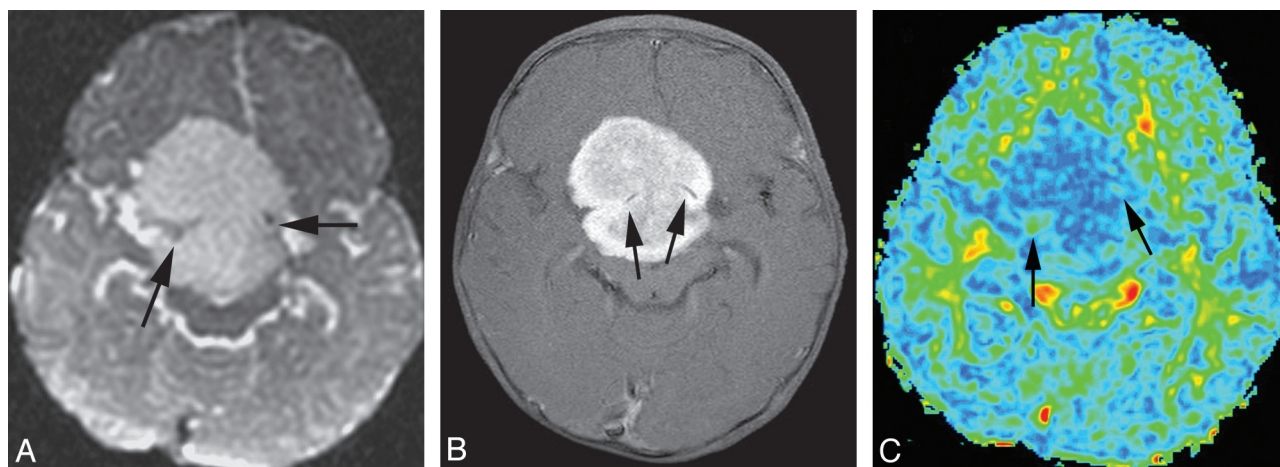

Fig 2. *A*, T2-weighted (*b* = 0) MR image shows a grade II glioma. *B*, Postgadolinium axial T1-weighted image shows whole-tumor contrast enhancement. *C*, FA map shows tumor FA with a homogeneous blue hue. The darker blue (cool color tone) represents low FA and the red and yellow (warm color tones) correspond to high FA. Region-of-interest selection for FA measurement is based on visually inspecting the hue. Maximum FA, minimum FA, FA range, and maximum SD are 0.145, 0.061, 0.084, and 0.0411, respectively. Arrows point to arteries.

We positioned the region of interest multiple times (usually in the range of 10–30 times) in each area of interest to make sure we measured the maximum/minimum FA or maximum SD of FA. The need to use a small region of interest for calculating maximum SDs is critical so that small areas of presumably very heterogeneous pathologic change would not be overlooked. These areas of high heterogeneity may be a small component of an otherwise very homogeneous low-grade tumor. This technique roughly correlates to the neuropathologic approach in which the grade of the tumor is based on the highest grade of tumor found, even if it is a very small component of the whole tumor.

When the contrast enhancement was small, punctate, or a thin ring, the FA for the enhanced component was not measured. When the enhanced and nonenhanced components were mixed and could not be evaluated separately, the FAs were only recorded as being from the whole tumor.

Statistical Analysis

Data analysis was performed by a biostatistician (F.Y.) by using a commercial statistical software, SAS, Version 9.2 (SAS Institute, Cary, North Carolina). FA measurements were quantitatively compared among different tumor grades and tumor components. Normality assumption was first checked for the FA measurements of each tumor grade and component. The minimum FA, the maximum FA, and the range of FA failed to meet the normal assumption. Accordingly, the ANOVA with unequal variance was used for overall comparison of the mean value of maximum SD and mean FA, respectively. Alternatively, the Kruskal-Wallis test, a nonparametric version of ANOVA, was used to compare the minimum FA, maximum FA, and FA range, respectively, among all grades and components. To evaluate differences between each pair of groups, we used the Tukey multiple comparison method. $P < .05$ was considered significant.

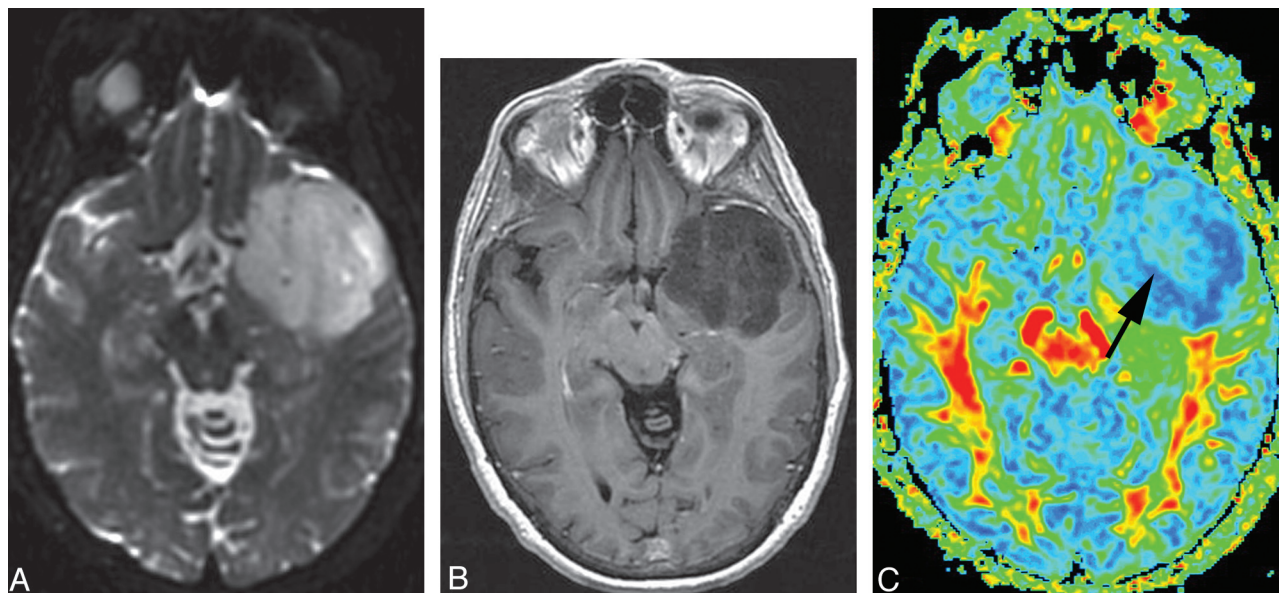When a significant difference was observed in a metric between

Fig 3. *A,* T2-weighted MR image shows a grade III glioma. *B,* Postgadolinium axial T1-weighted image does not show obvious tumor contrast enhancement. *C,* FA map shows that the tumor has a warmer color tone (light green [*arrow*]) compared with that in Fig 2. Maximum FA, minimum FA, FA range, and maximum SD are 0.170, 0.0794, 0.0906, and 0.0507, respectively. Each value of the measurements for this grade III tumor is correspondingly larger than that for the grade II tumor shown in Fig 2.

Fig 4. *A,* FLAIR image shows a grade IV glioma. *B,* Postgadolinium axial T1-weighted image shows inhomogeneous tumor contrast enhancement. *C,* FA map shows that the tumor has a warmer color tone (dark green and scattered yellow and red) compared with that in Figs 2 and 3. Maximum FA, minimum FA, FA range, and maximum SD are 0.346, 0.0834, 0.2626, and 0.11, respectively. Each value of the measurements for this grade IV tumor is correspondingly larger than that for the grade III tumor shown in Fig 3.
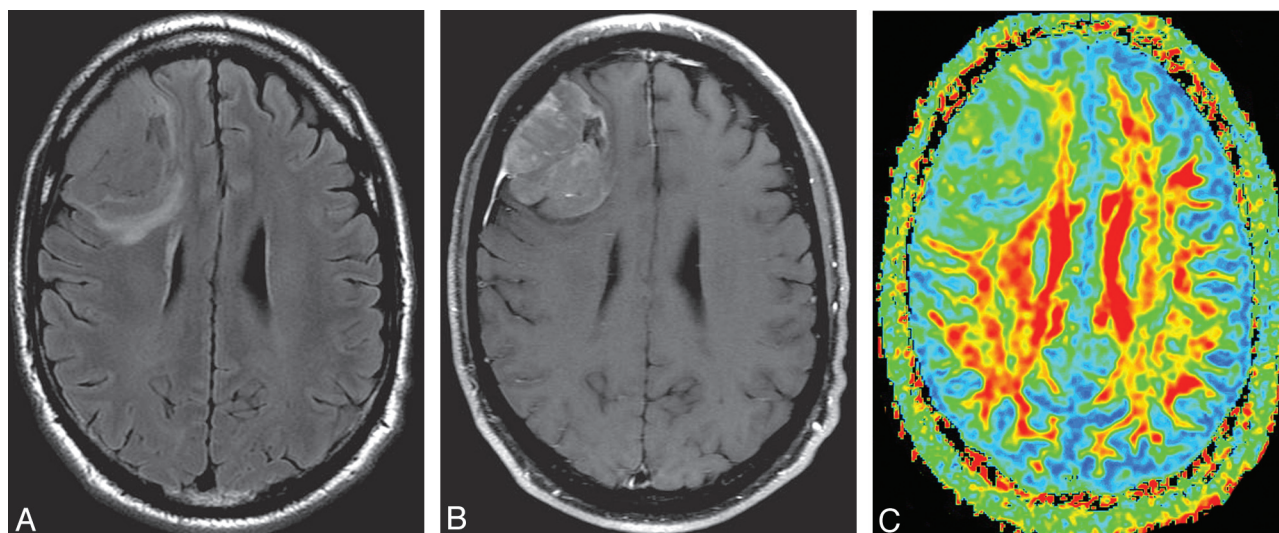
low-grade (II) and high-grade (III and IV) tumors, an ROC was further applied to identify the cutoff value of the metric that yielded the best combination of sensitivity and specificity, to distinguish low- and high-grade tumors.

We also correlated FA variations (FA range and maximum SD) with minimum FA and maximum FA. In addition, the effect of tumor size on the FA variation was assessed. Because the data were not normally distributed, a Spearman rank correlation was calculated for the evaluation.

Results

Conventional MR Imaging Findings

The mean maximum diameters of the tumors were 4.5 cm (range, 3–6.3 cm) for grade II, 6.1 cm (range, 3–9.2 cm) for grade III, and 4.9 cm (range, 2.7–8.0 cm) for grade IV tumors. Only 1 grade IV tumor was <3 cm with a maximum diameter of 2.7 cm. Contrast enhancement was noted in only 1 grade II tumor that was pathologically proved as a pilomyxoid astrocytoma. The enhancement was total and homogeneous. There was no cystic or necrotic change in the grade II tumors. Four grade III tumors were nonenhancing, and 4 had punctate nodular-like areas of contrast enhancement. One grade III tumor contained a cystic area. There was no obvious cystic or necrotic change in the other 7 grade III tumors. Irregular contrast enhancement was noted in all 17 grade IV tumors. Four grade IV tumors had nonenhanced tumor components. All grade IV tumors had various degrees of cyst formation and necrosis. Five of 8 grade III tumors were preoperatively diag-
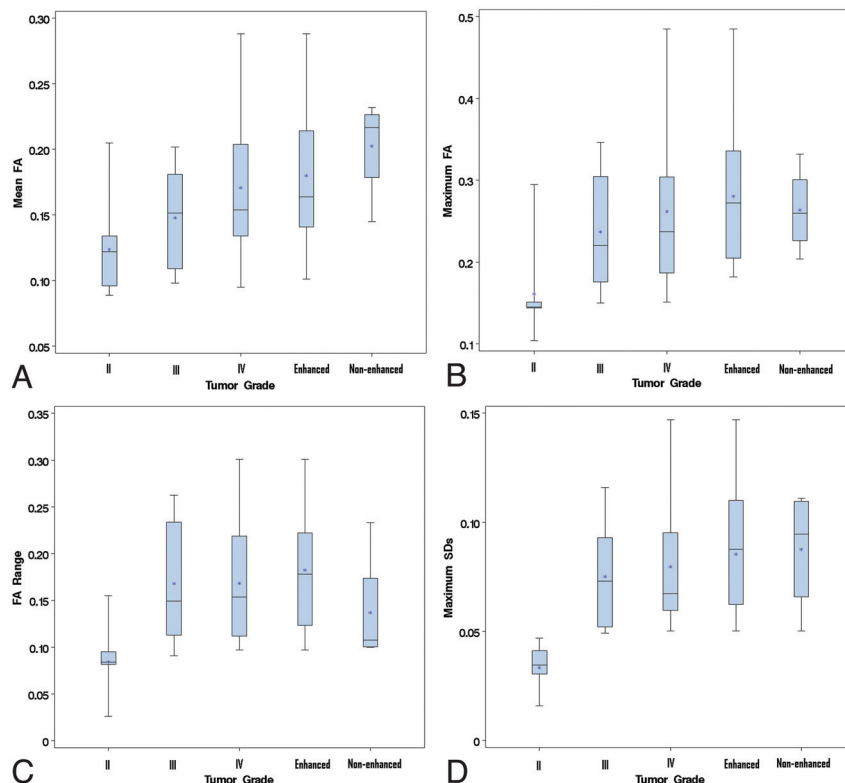
Fig 5. Graphs show the comparisons of FA measurements among tumor grades and components. Boxes represent the range between the first and third quartiles. Median values are shown as horizontal lines within each box. Asterisks indicate the mean value in each group. Vertical lines extending from the top and bottom of each box terminate at the maximum and minimum values, respectively. *A,* Mean FA for grade II tumors is lower than that for grade IV tumors, nonenhanced components, or enhanced components, respectively, with a significant or approaching significant difference. *B,* The maximum FA for grade II tumors is significantly lower than that for grade III, IV, or components. *C,* The FA range for grade II tumors is significantly lower than that for grade III, IV, or enhanced components. *D,* The maximum SD for grade II tumors is significantly lower than that for grade III, IV, or components. For all measurements, there was no significant difference among any pair of grade III, IV, or components.

nosed as low-grade gliomas, and the pilomyxoid astrocytoma was suspected to be a germinoma. The preoperative grading of all the other tumors (including grade II and IV) was consistent with histopathology. The sensitivity and specificity of conventional MR imaging in differentiating low-grade from high-grade (grade III and IV) tumors were 83.3% and 90%, respectively. However, the sensitivity and specificity of conventional MR imaging for differentiating grade II from grade III tumors were 61.5% and 90%, respectively.

Tumor FA Values

Only whole-tumor FA measurements were made in grade III tumors in which the contrast enhancement consisted of small nodules. Among grade IV tumors, 2 had mixed nonenhanced and enhanced components, and 2 had very small areas of enhancement. Therefore, 9 grade II tumors, 8 grade III tumors, 17 grade IV tumors, 4 nonenhanced components (grade IV), and 13 enhanced components (grade IV) were included for FA measurement. Only 4 nonenhanced components of grade IV tumors were identified for analysis because ambiguous non-enhancing areas of tumor versus edema were not included.

The ANOVA with unequal variance was used for comparison of the mean FA value among all grades and components. The mean FA value for grade II tumors (mean, 0.124 ± 0.035) was significantly lower than that for grade IV tumors (0.171 ± 0.054) ($P = .0363$) and nonenhanced components (0.203 ± 0.039) ($P = .0275$), but not significantly different from that for grade III tumors (0.148 ± 0.040) ($P = .4027$). The difference

between grade II tumors and enhanced components (0.180 ± 0.055) approached significance ($P = .0540$). There were no significant differences among any pair of grade III, IV, or components (Fig 5*A*).

Maximum and Minimum FA Values

The mean values of the maximum FAs were 0.161 ± 0.054 for grade II, 0.237 ± 0.073 for grade III, 0.262 ± 0.090 for grade IV, 0.264 ± 0.053 for nonenhanced components, and 0.280 ± 0.093 for enhanced components. By using the Kruskal-Wallis test, statistically significant differences were found between grade II and grade III ($P = .0164$), grade IV ($P = .0007$), the nonenhanced components ($P = .0187$), and the enhanced components ($P = .0007$). No significant difference was found among any pair of grade III, IV, or components (Fig 5*B*).

With regard to the mean value of the minimum FAs, no significant difference was found among any pair of grade II, III, or IV tumors.

FA Range

The Kruskal-Wallis test was used to compare the FA range among all grades and components. The FA range for grade II tumors (0.084 ± 0.036) was significantly lower than that for grade III (0.168 ± 0.067) ($P = .0034$), grade IV (0.168 ± 0.070) ($P = .0004$), and the enhanced component (0.182 ± 0.068) ($P = .0001$). We also observed that the FA range for grade II tumors was lower than that for the nonenhanced component (0.137 ± 0.064), close to significance ($P = .0692$).
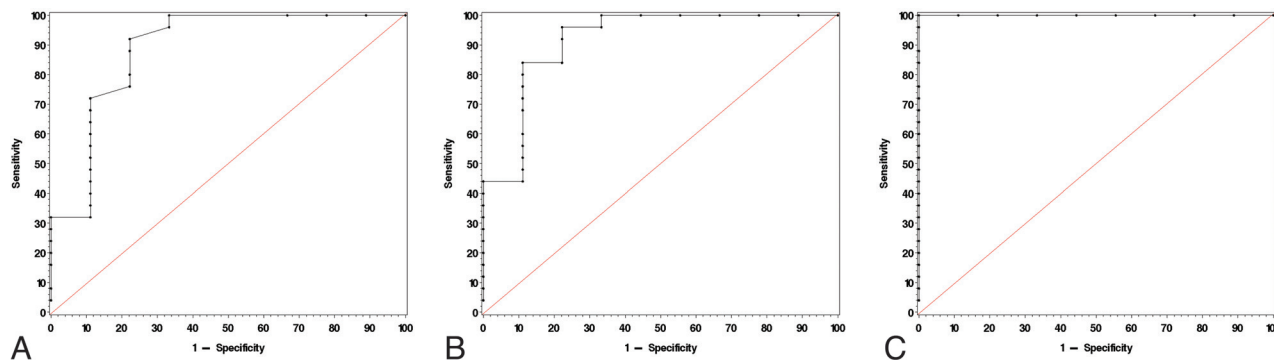
Fig 6. ROC curves use maximum FA (*A*, cutoff value = 0.17, sensitivity = 92%, specificity = 77.8%), FA range (*B*, cutoff value = 0.0971, sensitivity = 96%, specificity = 77.8%), and maximum SD (*C*, cutoff value = 0.0492, sensitivity = 100%, specificity = 100%) to differentiate grade II from grade III and IV gliomas.

No significant difference was found among any pair of grade III, IV, or components (Fig 5*C*).

A very good correlation (correlation coefficient = 0.931) between FA range and maximum FA was observed. In contrast, only a fair correlation (correlation coefficient = 0.409) was noted between FA range and minimum FA.

Maximum SD

The ANOVA with unequal variance was used for comparison of the maximum SDs among all grades and components. The mean values of the maximum SDs were 0.033 ± 0.011 for grade II, 0.075 ± 0.025 for grade III, 0.080 ± 0.028 for grade IV, 0.088 ± 0.028 for the nonenhanced components, and 0.085 ± 0.029 for the enhanced components. Statistically significant differences of the maximum SDs were found between grade II and grade III (P = .0008), grade IV (P < .0001), nonenhanced components (P = .0048), or enhanced components (P = .0305). No significant difference was found for maximum SD among any pair of grade III, IV, or components (Fig 5*D*). A very good correlation (correlation coefficient = 0.889) between maximum SD and maximum FA was observed. In contrast, only a fair correlation (correlation coefficient = 0.467) was noted between maximum SD and minimum FA.

No correlation was found between tumor size and FA variation with a correlation coefficient < 0.1.

Cutoff Value of FA from ROC

The cutoff value of 0.17 for the maximum FA differentiated low- from high-grade tumors with a sensitivity of 92% and a specificity of 77.8% (Fig 6*A*). The cutoff value for the FA range was 0.0971, which yields a sensitivity of 96% and a specificity of 77.8% (Fig 6*B*). The cutoff value of 0.0492 for the maximum SD had both a sensitivity and specificity of 100% and showed complete agreement with histopathologic grading (Fig 6*C*). As to differentiating grade II from grade III tumors, the cutoff values were set to 0.17, 0.109, and 0.0492 for the maximum FA, the FA range, and the maximum SD, respectively. The sensitivity and specificity were 87.5% and 77.8% for the maximum FA, 87.5% and 88.9% for the FA range, and both were 100% for the maximum SD.

Discussion

Our study revealed that the mean FAs were significantly higher in grade IV than in grade II gliomas. However, all the grade IV gliomas had cyst formation, necrosis, and/or irregular contrast enhancement in various degrees. None were preoperatively diagnosed as a lower grade glioma. By contrast, 5 of the 8 grade III gliomas were preoperatively diagnosed by conventional MR imaging as grade II gliomas due to benign imaging features. However, mean FA did not significantly differ between grade III and grade II gliomas either. Therefore, there was no added value of mean FA evaluation over conventional MR imaging in grading gliomas despite a mean FA difference between grade IV gliomas with typical malignant imaging features and grade II gliomas. A study by Inoue et al[6] showed that grade III gliomas had significantly higher FA than grade II gliomas. However, the FA values were measured within enhanced components when the tumor had contrast enhancement. In contrast, all the grade III gliomas in our study were nonenhanced or had miniscule contrast enhancement.

Tumor cells that infiltrate fiber tracts cause displacement, deviation, and destruction of these tracts and lead to reduction of FA. With more active tumor proliferation and consequently more obvious fiber tract disorganization, it might be hypothesized that high-grade gliomas are expected to reveal lower FA values than low-grade gliomas.[19-22] However, our result, higher mean FA values in high-grade gliomas, is contrary to this expectation. This difference could be explained by the increases of cell density, cellularity, and vascularity in high-grade gliomas. It has been previously reported that tumor FA positively correlates to cell density, cellularity, and vascularity.[11,12]

Sometimes high-grade gliomas, especially grade III, have focal hypercellularity and higher cell density within an otherwise low-grade-appearing mass.[15-17] The malignant foci might not be large enough to induce mean FA changes in the whole tumor but could induce higher FA values in these foci. In our study, the mean values of maximum FA of both grade III and IV gliomas were significantly higher than those of grade II gliomas.

When comparing minimum FAs, we found no difference between low- and high-grade gliomas. This could be attributed to the fact that most high-grade gliomas arise from dedifferentiated lower grade ones.[15-17] The low-grade glioma tissue, which has low FA values to start with, is likely due to less cellularity and density and may still exist in high-grade gliomas.

Like maximum FA, the FA range and maximum SD in grade II gliomas were significantly smaller than those in grade

IV gliomas with typical malignant features as well as in the grade III gliomas with benign findings on conventional imaging. A strong correlation of maximum FA with FA range and maximum SD was noted statistically. Our study suggested that the larger FA ranges and maximum SDs in higher grade gliomas might be mainly caused by the increased maximum FA values. Because most grade III gliomas in this study were lacking in malignant features on conventional imaging, the difference of maximum FA, FA range, and maximum SD between grade II and III gliomas in our study population provided added value to conventional MR imaging in the differentiation of these tumors. By using the specified cutoff values of maximum FA, maximum SD, and FA range, ROC revealed that the sensitivities increased from 61.5% on conventional imaging to 87.5%–100% in differentiating grade II from grade III gliomas and from 83.3% to 92%–100% in differentiating grade II from grade III and IV gliomas, respectively. This finding is also clinically significant because of the dramatically different treatment and prognosis between the low- and high-grade gliomas.[23,24] Further study with more cases is necessary to evaluate the ROC in a larger population. We were not able to evaluate FA characteristics in patients with highly enhancing grade III gliomas because the grade III gliomas in this study were nonenhancing or had only punctuate nodular-like areas of contrast enhancement.

Theoretically, the larger the tumor, the more likely it is to have more areas of histologic variability. A large low-grade glioma could potentially have greater FA variation than a small high-grade glioma. However, only 1 high-grade glioma was <3 cm in this study. Given this finding, we were not able to specifically compare the FA variation between large low-grade gliomas and small high-grade gliomas. When analyzing all our cases, we found no correlation between tumor size and FA variation.

To our knowledge, there has been very limited analysis of heterogeneity using diffusion imaging in gliomas. In 1 study, the analysis focused on apparent diffusion coefficient values but did point to a potential broader application of our tumor analysis approach.[25] In another study, visual FA map analysis was used and grade II tumors were homogeneous but overall FA evaluation did not help grade tumors.[26] Our analytic approach of evaluating focal maximum SD is rudimentary at this point, but the results are promising.

We speculate that the tumor components with maximum SD or high maximum FA might reflect regional heterogeneity of histopathology and/or the more malignant foci. The need to define focal changes in a glioma rather than average values of metrics can be very important because a small focal area of high-grade glioma in an otherwise low-grade glioma makes a critical diagnostic difference. Our approach of focal SD analysis lends itself to creating maps of the SD metrics in a mass by calculating the focal SD across a lesion on a pixel-by-pixel basis. This SD map could then provide guidance for further noninvasive analysis or even biopsy. Of course, the point of maximum FA in a glioma may also provide a target for biopsy and directed neuropathologic analysis. However, future studies correlating diffusion tensor imaging to tissue histopathology are needed to confirm this speculation.

Positive correlation between FA and vascularity has been reported previously.[11] However, no significant difference of FA was found among nonenhanced and enhanced high-grade tumors or components in this study. This is likely because tumor enhancement results mainly from disruption of the blood-brain barrier, not tumor vascularity.[27,28] Our FA evaluation of the nonenhanced tumor components of grade IV tumors was likely affected by the fact we did not include areas in the brain that had high T2-weighted signal intensity but were ambiguous for representing tumor or only edema. This limited our analysis of nonenhanced components of grade IV tumors to $n = 4$.

There were limitations to our study. The results were obtained on the basis of a small number of patients. Some patients only had biopsies that could be associated with the potential for tumor undergrading. On the other hand, the regions of interest for measuring maximum FA and SD were not assessed histologically. Therefore, we can only speculate that areas with maximum FA might be the most metabolically active portions of tumor, which have hypercellularity, higher cell density, and increased vascularity. Also, we can only speculate that maximum SD might represent regional heterogeneity of histopathology. In applying our technique more broadly, we found that obtaining an accurate FA measurement is also likely limited in small tumors or very infiltrative tumors because the FA values of these tumors would likely be markedly affected by infiltrating white matter fibers. Region-of-interest mismapping may have occurred when evaluating the FA characteristics of the whole tumors and the tumor components and when avoiding areas of cysts, necrosis, and hemorrhage. If mismapping occurred, then the FA values measured would not be representative of the soft-tissue components that we were aiming to measure. Because we carefully placed the regions of interest on the basis of multiple MR imaging sequences, we have minimized the potential for such errors.

Conclusions

The results of this study reveal that high-grade gliomas have a greater variation of FA values. In addition, focal maximum FA, the key factor for causing larger FA variation, itself appears useful in differentiating glioma grades. Further study that correlates maximum FA and maximum SD with histologic features is needed to make definite conclusions about the clinical application of these diffusion tensor metrics in grading gliomas.

References

1. Osborn AG. **Astrocytomas and other glial neoplasms.** In: Patterson AS, ed. *Diagnostic Neuroradiology.* St. Louis: Mosby; 1994:529–78
2. Louis DN, Ohgaki H, Wiestler OD, et al. **The 2007 WHO classification of tumors of the central nervous system.** *Acta Neuropathol* 2007;114:97–109. Epub 2007 Jul 6.
3. Ginsberg LE, Fuller GN, Hashmi M, et al. **The significance of lack of MR contrast enhancement of supratentorial brain tumors in adults: histopathological evaluation of a series.** *Surg Neurol* 1998;49:436–40
4. White ML, Zhang Y, Kirby P, et al. **Can tumor contrast enhancement be used as a criterion for differentiating tumor grades of oligodendrogliomas?** *AJNR Am J Neuroradiol* 2005;26:784–90
5. Okamoto K, Ito J, Takahashi N, et al. **MRI of high-grade astrocytic tumors: early appearance and evolution.** *Neuroradiology* 2002;44:395–402
6. Inoue T, Ogasawara K, Beppu T, et al. **Diffusion tensor imaging for preoperative evaluation of tumor grade in gliomas.** *Clin Neurol Neurosurg* 2005;107:174–80
7. Stadlbauer A, Ganslandt O, Buslei R, et al. **Gliomas: histopathologic evaluation of changes in directionality and magnitude of water diffusion at diffusion-tensor MR imaging.** *Radiology* 2006;240:803–10

8. Tropine A, Vucurevic G, Delani P, et al. **Contribution of diffusion tensor imaging to delineation of gliomas and glioblastomas.** *J Magn Reson Imaging* 2004;20:905–12

9. Lee HY, Na DG, Song IC, et al. **Diffusion-tensor imaging for glioma grading at 3-T magnetic resonance imaging: analysis of fractional anisotropy and mean diffusivity.** *J Comput Assist Tomogr* 2008;32:298–303

10. Goebell E, Paustenbach S, Vaeterlein O, et al. **Low-grade and anaplastic gliomas: differences in architecture evaluated with diffusion-tensor MR imaging.** *Radiology* 2006;239:217–22

11. Beppu T, Inoue T, Shibata Y, et al. **Measurement of fractional anisotropy using diffusion tensor MRI in supratentorial astrocytic tumors.** *J Neurooncol* 2003;63:109–16

12. Beppu T, Inoue T, Shibata Y, et al. **Fractional anisotropy value by diffusion tensor magnetic resonance imaging as a predictor of cell density and proliferation activity of glioblastomas.** *Surg Neurol* 2005;63:56–61

13. Goebell E, Fiehler J, Ding XQ, et al. **Disarrangement of fiber tracts and decline of neuronal density correlate in glioma patients: a combined diffusion tensor imaging and 1H-MR spectroscopy study.** *AJNR Am J Neuroradiol* 2006;27:1426–31

14. Sijens PE, Heesters MA, Enting RH, et al. **Diffusion tensor imaging and chemical shift imaging assessment of heterogeneity in low grade glioma under temozolomide chemotherapy.** *Cancer Invest* 2007;25;706–10

15. Louis DN, Reifenberger G, Brat DJ, et al. **Tumors: introduction and neuroepithelial tumors.** In: Love S, Louis DN, Ellison DW, eds. *Greenfield's Neuropathology.* 8th ed. London, UK: Hodder Arnold; 2008:1821–936

16. Jayaraman MV, Boxerman JL. **Adult brain tumors.** In: Atlas SW, ed. *Magnetic Resonance Imaging of the Brain and Spine.* 4th ed. Philadelphia: Lippincott Williams & Wilkins; 2009:445–504

17. VandenBerg SR. **Current diagnostic concepts of astrocytic tumors.** *J Neuropathol Exp Neurol* 1992;51:644–57

18. Nafe R, Van de Nes J, Yan B, et al. **Distribution of nuclear size and internuclear distance are important criteria for grading astrocytomas.** *Clin Neuropathol* 2006;25:48–56

19. Roberts TP, Liu F, Kassner A, et al. **Fiber density index correlates with reduced fractional anisotropy in white matter of patients with glioblastoma.** *AJNR Am J Neuroradiol* 2005;26:2183–86

20. Sinha S, Bastin ME, Whittle IR, et al. **Diffusion tensor MR imaging of high-grade cerebral gliomas.** *AJNR Am J Neuroradiol* 2002;23:520–27

21. Witwer BP, Moftakhar R, Hasan KM, et al. **Diffusion-tensor imaging of white matter tracts in patients with cerebral neoplasm.** *J Neurosurg* 2002;97:568–75

22. Wieshmann UC, Symms MR, Parker GJ, et al. **Diffusion tensor imaging demonstrates deviation of fibres in normal appearing white matter adjacent to a brain tumour.** *J Neurol Neurosurg Psychiatry* 2000;68:501–03

23. Philippon JH, Clemenceau SH, Fauchon FH, et al. **Supratentorial low-grade astrocytomas in adults.** *Neurosurgery* 1993;32:554–59

24. Walker MD, Green SB, Byar DP, et al. **Randomized comparisons of radiotherapy and nitrosoureas for the treatment of malignant glioma after surgery.** *N Engl J Med* 1980;303:1323–39

25. Chang SM, Nelson S, Vandenberg S, et al. **Integration of preoperative anatomic and metabolic physiologic imaging of newly diagnosed glioma.** *J Neurooncol* 2009;92:401–15

26. Ferda J, Kastner J, Mukenšnabl P, et al. **Diffusion tensor magnetic resonance imaging of glial brain tumors.** *Eur J Radiol* 2010;74:428–36

27. Kurki T, Lundbom N, Kalimo H, et al. **MR classification of brain gliomas: value of magnetization transfer and conventional imaging.** *Magn Reson Imaging* 1995;13:501–11

28. Scott JN, Brasher PM, Sevick RJ, et al. **How often are nonenhancing supratentorial gliomas malignant? A population study.** *Neurology* 2002;59:947–49